

See discussions, stats, and author profiles for this publication at:
<https://www.researchgate.net/publication/244327521>

Theoretical study of the solvatochromism of a merocyanine dye

ARTICLE in CHEMICAL PHYSICS · NOVEMBER 1997

Impact Factor: 1.65 · DOI: 10.1016/S0301-0104(97)00234-6

CITATIONS

9

READS

41

2 AUTHORS:



Sebastian Fernandez-Alberti

National University of Quilmes

46 PUBLICATIONS 697 CITATIONS

SEE PROFILE



Julian Echave

National University of General San Ma...

69 PUBLICATIONS 1,601 CITATIONS

SEE PROFILE

Theoretical study of the solvatochromism of a merocyanine dye

Sebastián Fernández Alberti^{*}, Julián Echave

Centro de Estudios e Investigaciones, Universidad Nacional de Quilmes, Saenz Peña 180, 1876 Bernal, Argentina

Received 20 May 1997

Abstract

Molecular dynamics (MD) simulations of a strongly polar merocyanine dye in solutions with acetone and methanol were performed using a quantum mechanical/molecular mechanical (QM/MM) mixed model. The solute was represented by its zwitterion and quinone resonance forms. The 102 nm blue shift of the UV–visible absorption band observed when the dye is transferred from acetone to methanol was analysed. Semiempirical electronic structure calculations on configurations obtained randomly from the data collection period of the MD run were used to study the effect of the solvent on the UV–visible spectrum. Different levels of solvent representation were considered: a self-consistent reaction field (SCRF) approach, a QM/MM mixed model and a solute–solvent supermolecule model. The semiempirical method AM1 was employed to calculate absolute energies, dipole moments and solute partial charges during the dynamics, whereas another semiempirical method, ZINDO/S, was employed to obtain the electronic spectra. The solvents considered have very similar polarities and therefore their solvatochromic effects are due mainly to specific interactions. Accordingly, we found that only the supermolecule model is able to predict the observed blue shift, that turns out to be produced by the effect of the first solvation shell over the zwitterion resonant form, that predominates over the quinone in both solvents. A detailed analysis of zwitterion–solvent specific interactions suggests that a nucleophile–carbonyl interaction in acetone and a hydrogen bond in methanol would be the main causes of the solvatochromism. © 1997 Elsevier Science B.V.

1. Introduction

The solvatochromic properties of merocyanines were first reported by Brooker et al. [1,2]. The strongly polar ones show a large hypsochromic (blue) shift in their UV–visible absorption bands with increasing solvent polarity. In the present work we consider the very polar merocyanine, 2-(2-(4-hydroxyphenyl)-ethenyl)-1-methylpyridinium, that we shall call MC from now on. This dye shows one of

the largest known solvatochromic effects among merocyanines, with a variation in absorption wavelength, λ_{\max} , between 620 nm in CHCl_3 and 442 nm in H_2O [3,4].

The solvatochromism of MC has been the subject of several theoretical studies [5–8]. The most accepted interpretation is that MC is a resonant mixture of zwitterion and quinone (Fig. 1), and the wavelength shift is due to an increase in the contribution of the zwitterion with solvent polarity.

Early semiempirical calculations have modelled the solvated O and N atoms of MC by using linear combinations of the nonsolvated semiempirical pa-

^{*} Corresponding author. Present address: IRSAMC-LCAR, 118 route de Narbonne, F-31062 Toulouse Cedex 4, France.

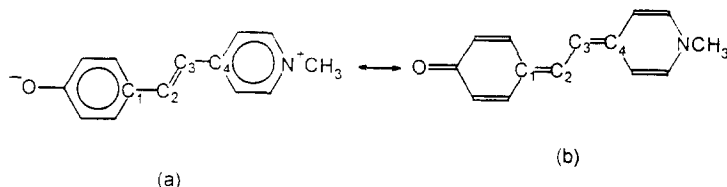


Fig. 1. Solute resonance forms. Zwitterion (a) and quinone (b) valence structures.

rameters for OH and O, and NH and N, respectively [5]. Clearly, implicit in this model is the assumption that the only relevant solute–solvent interactions occur at the level of these atoms. A later study, made use of the virtual-charge model of Constanciel and Tapia [9,6]. The model takes into account only non-specific solvent effects. Both techniques agree in the observation of a structure change from quinone to zwitterion accompanying the blue shift of the absorption band with increasing solvent polarity. More recently, the self-consistent reaction field (SCRF) approach as applied by Karelson and Zerner [10] was employed [7]. The reaction field turns out to be too small to reproduce the experimental solvatochromic behaviour of MC if the radius of the spherical solvent cavity is taken sufficiently large to include all the MC atoms inside it, while it works well for smaller but less realistic cavity radius.

None of the studies mentioned above considered the solvent explicitly. Luzhkov and Warshel used a Langevin dipoles method, in which the solvent, modelled as a set of polarizable dipoles, is incorporated into a semiempirical solute Hamiltonian [11]. Within this model, the experimentally observed solvent shift between water and pyridine could be reproduced, if MC's zwitterion predominates in both solvents. It is worthwhile to note that this result is in contrast with the above-mentioned treatments in which the solvatochromism is accompanied by a gradual change in zwitterion/quinone ratio with solvent polarity.

From the above paragraphs it follows that the origin of MC's solvatochromism is not at all clear. Besides, we will show that an explicit inclusion of the solvent in the electronic spectra calculations is necessary to study the effect of possible specific solute–solvent interactions, that empirical studies using Linear Solvent Energy Relationships (LSER) [12,13] suggest are very important. In order to study

specific effects we chose methanol and acetone, because they have very similar nonspecific effects, but very different specific ones. Thus, they have similar values of the LSER π^* parameter (0.60 and 0.71, respectively), that measures dispersive, inductive, and electrostatic interactions, whereas they have very different values of the α parameter (0.98 and 0.0, respectively), that reflects solvent hydrogen bond donor acidities.

In the present work, we study the solvatochromism of MC in acetone and methanol using different levels of representation of the solvent, in order to verify the importance of specific effects and to assess which kind of theoretical approaches can be used to study this kind of system.

The paper is organized as follows: In Section 2 we describe the models and the methods used. In Section 3 we present and discuss our results. Finally, in Section 4 we summarise our findings.

2. Models and methods

Basically, we have considered four systems: each of the resonance forms of MC, zwitterion and quinone, into each of the two solvents methanol and acetone. For each system we performed an MD run, using a mixed model in which a molecular mechanics (MM) force field is used for solvent–solvent and solvent–solute interactions, while the solute's partial charges are calculated quantum mechanically during the classical trajectory calculation. Once the MD run was over, we chose some configurations at random from the data collection period to perform semiempirical calculations of the electronic spectrum using different levels of solvent representation.

2.1. Solvents

Both solvents were modelled using the united atoms OPLS/Amber force field because it was shown that it reproduces these liquid phases correctly and it gives a good description of the hydrogen bond interactions in the liquid methanol [16,28,14]. This field combines Amber's intramolecular interactions [14] with intermolecular interactions calculated using OPLS potentials [16,17]. Methyl groups are represented by a single interaction site center on the carbon atom. In Tables 1 and 2 we show the potential parameters used.

We performed MD simulations for the pure solvents, using the NVT ensemble with $T = 298$ K, employing the experimental densities [18,19]. The systems were coupled to a constant temperature bath with bath coupling $\tau_T = 0.2$ ps [20]. Periodic boundary conditions were applied. The leap frog algorithm with a time step of 0.001 ps was used to integrate the equations of motion. After enough time for equilibration, we collected data every 0.01 ps during 100 ps. Box sizes between 20 and 24 Å were used in order to check convergence.

Table 1
OPLS parameters [15,16]

Methanol:	
q_{CH_3} (e)	0.265
q_{O} (e)	−0.700
q_{H} (e)	0.435
$\epsilon_{\text{CH}_3\text{CH}_3}$ (kcal/mol)	0.207
ϵ_{OO} (kcal/mol)	0.170
$\sigma_{\text{CH}_3\text{CH}_3}$ (Å)	3.775
σ_{OO} (Å)	3.070
Acetone:	
q_{CH_3} (e)	0.062
q_{O} (e)	−0.424
q_{C} (e)	0.300
$\epsilon_{\text{CH}_3\text{CH}_3}$ (kcal/mol)	0.160
ϵ_{OO} (kcal/mol)	0.210
ϵ_{CC} (kcal/mol)	0.105
$\sigma_{\text{CH}_3\text{CH}_3}$ (Å)	3.910
σ_{OO} (Å)	2.960
σ_{CC} (Å)	3.750

Table 2
Amber parameters [14]

Methanol		
Bond	r_{eq} (Å)	K_r (kcal mol ^{−1} Å ^{−3})
CH ₃ O	1.425	386.0
OH	0.96	553.0
Angle	θ_{eq} (°)	K_θ (kcal mol ^{−1} rad ^{−2})
CH ₃ OH	108.5	55.0
Acetone		
Bond	r_{eq} (Å)	K_r (kcal mol ^{−1} Å ^{−3})
CH ₃ C	1.522	317.0
CO	1.229	570.0
Angle	θ_{eq} (°)	K_θ (kcal mol ^{−1} rad ^{−2})
CH ₃ CO	120.4	80.0

2.2. Solute + solvent

The quinone was obtained by geometry optimization in vacuo with the semiempirical method AM1 [21]. To obtain the zwitterion form we optimised the protonated MC. Then, we removed the H⁺ and recalculated the charges using AM1 on this fixed geometry. The final zwitterion geometry is in good agreement with the one used by Luzhkov and Warshell [11], besides, the alternation of single and double bond agrees well with the intuitive idea of the zwitterion in this molecule. Furthermore, we should note that rather than the precise geometry it is important to represent MC's geometry change with solvent polarity [1–11]. We used AM1 because it predicts correctly molecular geometries as well as total energies and dipole moments [22]. Besides, AM1 has been used to study MC, and showed reasonable results for both resonant structures [8].

As we said before we considered four solute–solvent systems: zwitterion–acetone, quinone–acetone, zwitterion–methanol, and quinone–methanol. Each system consists of one solute molecule surrounded by solvent molecules (109 for acetone and 143 for methanol). We have used 20 × 20 × 25.41 Å³ boxes with a cut-off of 9 Å for acetone and 23 × 23 × 25.41 Å³ boxes with a cut-off

of 10.5 Å for methanol. As in the case of pure solvents, the systems were coupled to an external bath of $T = 298$ K with $\tau_T = 0.2$ ps, and the integration time step was 0.001 ps.

While the solvents were allowed to vibrate in the united atoms OPLS/Amber force field, the solutes were kept frozen during the dynamics. The initial solvent configuration was obtained by energy minimisation and then the optimised system was heated from 0 to 298 K in 10 ps.

Each MD run was split into two parts. First, we run 50 ps keeping fixed the partial charges of the solute, obtained from the AM1 calculations in vacuo as described above. Then, from that stabilised system we started a second type of calculation in which a combined QM/MM potential was employed. This calculation treated the solute quantum mechanically while the solvent was simulated using OPLS/Amber force field. The distribution of the point charges on the solvent atoms (classical region) affects the partial charges of the solute molecule (quantum mechanical region), that in turn affects the dynamics. In this way the QM/MM mixed model allows the inclusion of the polarization of the solute. The solute's partial charges were updated every 0.01 ps. This time is shorter than the velocities relaxation time τ_{relax} for both pure solvents, that is, the time it takes for the diffusional regime to dominate the motion. Shorter times were used as well to verify that the results were converged. This second part of the run was continued for 50 ps, of which 20 ps were required for a new equilibration.

In the QM/MM treatment [23] the solute was modelled using an AM1 Hamiltonian with a correction due to the interaction between the QM region (the solute) and the MM region (the solvent):

$$\Delta H_{\mu\nu} = - \sum_B (Z_B - Q_B) \gamma_{\mu\nu}^{AB}$$

with $\gamma_{\mu\nu}^{AB}$ the two-electron two center repulsion integral:

$$\gamma_{\mu\nu}^{AB} = \int \int \phi_\mu^A(1) \phi_\nu^A(1) \frac{1}{r_{AB}} s^B(2) s^B(2) d\tau_1 d\tau_2$$

where A is the index for an atom in the QM region and B for an atom in the MM region, $d\tau_1$ and $d\tau_2$

are the volume elements for the individual electrons 1 and 2, respectively, both ϕ_μ^A and ϕ_ν^A are atomic orbitals centered at atom A and s^B indicates an s-type atomic orbital on atom B, r_{AB} is the distance between A and B, Z_B is the core charge of atom B and Q_B is the electronic charge.

The interaction energy between the nuclei in the QM region and the partial charges in the MM region is:

$$\begin{aligned} \Delta E_N &= \sum_{(A,B)} \left\{ Z_A Z_B (s_A s_A | s_B s_B) \right. \\ &\quad \times \left[1 + \exp(-\alpha_A r_{AB}) + \frac{\exp(-\alpha_A r_{AB})}{R_{AB}} \right] \\ &\quad \left. - Z_A Q_B (s_A s_A | s_B s_B) \right\} \end{aligned}$$

with

$$(s_A s_A | s_B s_B) = \frac{1}{\left[r_{AB}^2 + \frac{1}{2} \left(\frac{1}{AM_A} + \frac{1}{AM_B} \right)^2 \right]^{1/2}}$$

where AM are the monopole–monopole interaction parameters and α_A a parameter of atom A.

2.3. UV-visible spectra

To obtain the UV-visible spectra we performed singly excited configuration interaction (CI) calculations with the semiempirical method ZINDO/S [24–27]. This model has been parametrized at the singly excited CI level to be accurate in the prediction of low-lying π – π^* bands and n – π^* bands in molecules containing H and elements of the first and second row.

We have considered three levels of solvent representation. First, we have used the self-consistent reaction field (SCRF) approach as applied by Karelson and Zerner. [10] The solute is placed in a spherical cavity immersed in a dielectric continuum characterized by its dielectric constant. Cavities of different sizes ranging from 6.0 to 9.0 Å were used

without observing significant differences in the UV–visible spectra in the range of solvent polarity we have studied. We finally used a cavity radius of 8.0 Å in order to compare the results with those of the supermolecule model described below. Second, we used a mixed QM/MM model similar to the one used for the MD run, but based on ZINDO/S [23]. This method treats the charges in the classical region in the following way:

$$\Delta H_{\mu\mu} = - \sum_B (Z_B - Q_B) \gamma_{\mu\mu}^{AB}$$

corrects the solute's core Hamiltonian element $H_{\mu\mu}$, and

$$\Delta E_N = \sum_{(A,B)} \left(\frac{Z_A Z_B}{r_{AB}} - Z_A Q_B \gamma_{ss}^{AB} \right)$$

corrects the interaction energy between the quantum mechanical nuclei and classical charges, where

$$\gamma_{ss}^{AB} = \frac{f_r}{\frac{2f_r}{\gamma_{ss}^A + \gamma_{ss}^B} + r_{AB}}$$

is the two-electron two center repulsion integral, $f_r = 1.2$ is a constant, and γ_{ss}^A and γ_{ss}^B are two-electron one-center repulsion integrals and they are semiempirical parameters required by the ZINDO/S model.

Finally, we have applied the same SCRF described previously but to a supermolecule formed by the solute molecule and all solvent molecules within a sphere of radius 8.0 Å and center at the C2 atom of MC. This cavity radius lets us incorporate at least the first solvation shell of MC. The distribution of solvent molecules around the solute was obtained from the MD run, as described below.

The QM/MM and supermolecule models were applied to configurations obtained randomly from the data collection period of the MD run. The number of configurations used was chosen to get converged averaged results. It is important to note at this point, that if the solute–solvent system is optimized by minimising its energy using AM1 the solvent tends to be repelled from the solute to distances too large for it to have a significant effect on the electronic spectrum. This is why it is necessary to obtain the solvent configurations from the MD runs, where

the solvent comes close enough to the solute to have an effect over its electronic structure.

3. Results and discussion

3.1. Equilibrium simulations

3.1.1. Pure solvents

The structural and dynamic properties of the solvent were analysed as a preliminary to the simulations of the solutions. This allowed us to check the representation of the solvents and compare with results obtained using rigid models [16,28].

Comparing cubic boxes of sizes between $L = 20$ and 24 Å we found convergent results for $L = 20$ Å for methanol and $L = 23$ Å for acetone. We calculated the translational self-diffusion coefficients, D , from the mean squared displacement via the Einstein relation and from the time integral of the velocity autocorrelation function of the centers of mass $C_v(t)$ (Fig. 2). For methanol, we obtained $D = (1.4 \pm 0.2) \times 10^{-5}$ cm²/s, somewhat lower than the experimental value and that obtained using rigid models [16]. For acetone we found $D = (3.8 \pm 0.3) \times 10^{-5}$ cm²/s, in good agreement with previous results [28]. These diffusion coefficients correspond to velocity relaxation times τ_{relax} of 0.020 ps for methanol and 0.087 ps for acetone.

Fig. 3 shows radial distribution functions for acetone and methanol. In the case of methanol, they are in good agreement with those reported by Jorgensen for the rigid model [16]. The integration of the first peaks of $g_{\text{OO}}(r)$ and $g_{\text{OH}}(r)$ for methanol gives 2.01 and 0.99, respectively. This means that each molecule participates in two hydrogen bonds, in one as a donor and in the other as an acceptor. In the case of acetone, the distributions show that there is less short-range structure, as is expected from the lack of hydrogen bonds.

3.1.2. Merocyanine in solvent

In Figs. 4 and 5 we show contour plots of the radial–angular distributions of solvent molecules around some atoms of the solute $f(r, \theta)$. The variable r is the length of the vector \vec{r} that joins the reference atom with the center of mass of the solvent

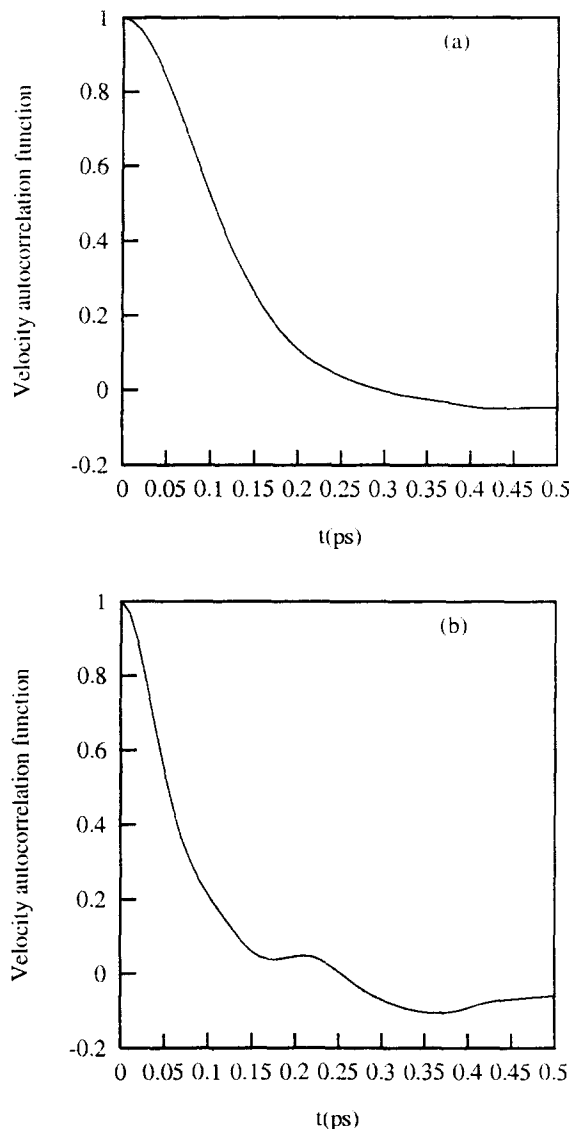


Fig. 2. Acetone (a), methanol (b) velocity autocorrelation functions of the centres of mass C_v .

molecule, whereas θ is the angle between \vec{r} and the solvent electric dipole. A fairly strong orientation of the solvent around certain solute sites was detected. Furthermore, significant differences were noted between quinone and zwitterion. For the quinone, the atoms with the most structured first solvation shells, either in acetone or methanol, are C1, C2, C3 and

C4, in the central part of the molecule. On the other hand, for the zwitterion the most structured first solvation shells are those of O and N.

The most localised first solvation shell is that of the O of the zwitterion in methanol. The first peak of its angular-radial distribution lies at $r = 2.9 \pm 0.2$ Å and has an angular range $[53.13^\circ, 78.46^\circ]$ with a

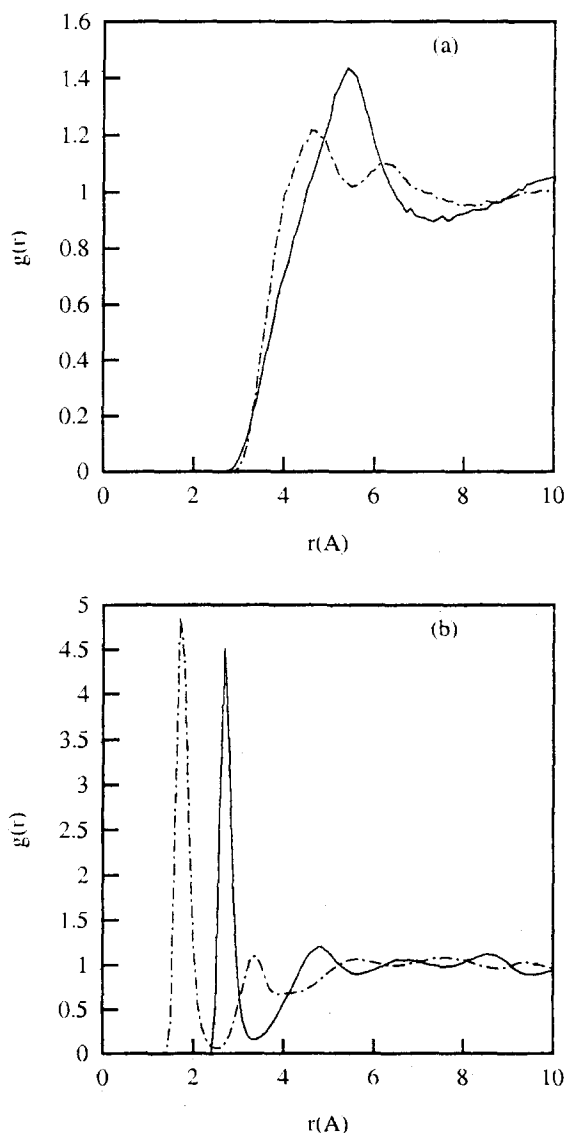


Fig. 3. (a) OO (—) and OC (---) radial distribution functions for acetone; (b) OO (—) and OH (---) radial distribution functions for methanol.

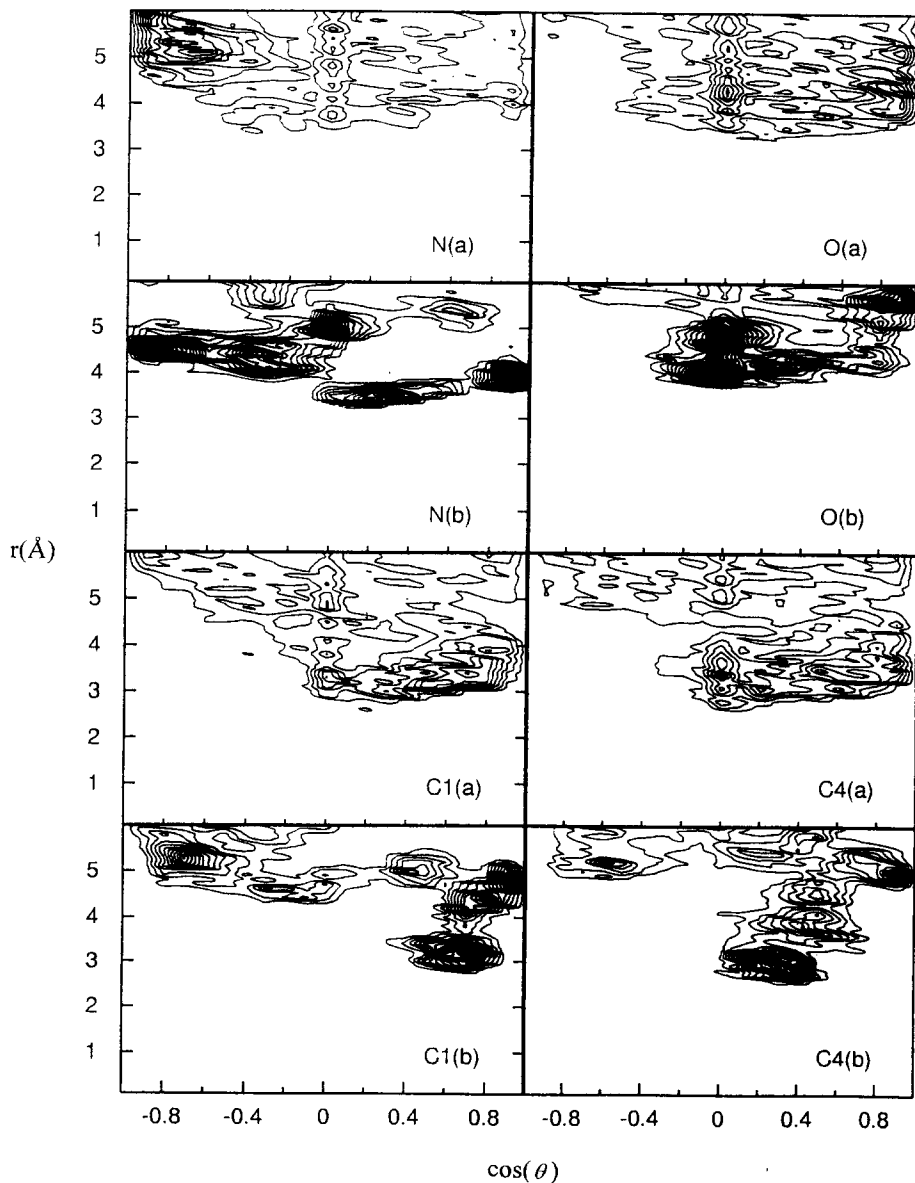


Fig. 4. Contour plots of the radial-angular distribution functions $f(r, \theta)$ of (a) acetone and (b) methanol dipoles around some quinone atoms.

maximum at 66.42° . These values correspond to a distance $O(MC)-O(Met)$ of 2.24 ± 0.2 Å (we use the notation $A(X)$ for atom A in molecule X) and an angle $H(Met)-O(Met)-O(MC)$ in the range $[3.85^\circ, 29.19^\circ]$ with a maximum at 17.15° . These values fall within the definition of a hydrogen bond in methanol

[29]. In agreement with this, the integration of the first peak (at 1.7 Å) of the radial distribution $g_{O(MC)H(Met)}(r)$ gives 2.23, which shows that an average of two molecules of methanol in the first solvation shell are hydrogen bonded to the zwitterion all through the MD.

3.2. Solvatochromism

In Table 3 we show the results of absorption spectra obtained employing different levels of solvent representation. This table shows that neither the SCRF method, nor the QM/MM one are able to reproduce the observed solvatochromic shift. Apply-

ing the SCRF method has very little effect on the absorption wavelength of either quinone or zwitterion. As in vacuo, the zwitterion gives a larger λ than the quinone. This is in opposition with the most accepted explanation of the experimental hypsochromic shift by an increase in the zwitterion's contribution in more polar solvents. The fact that

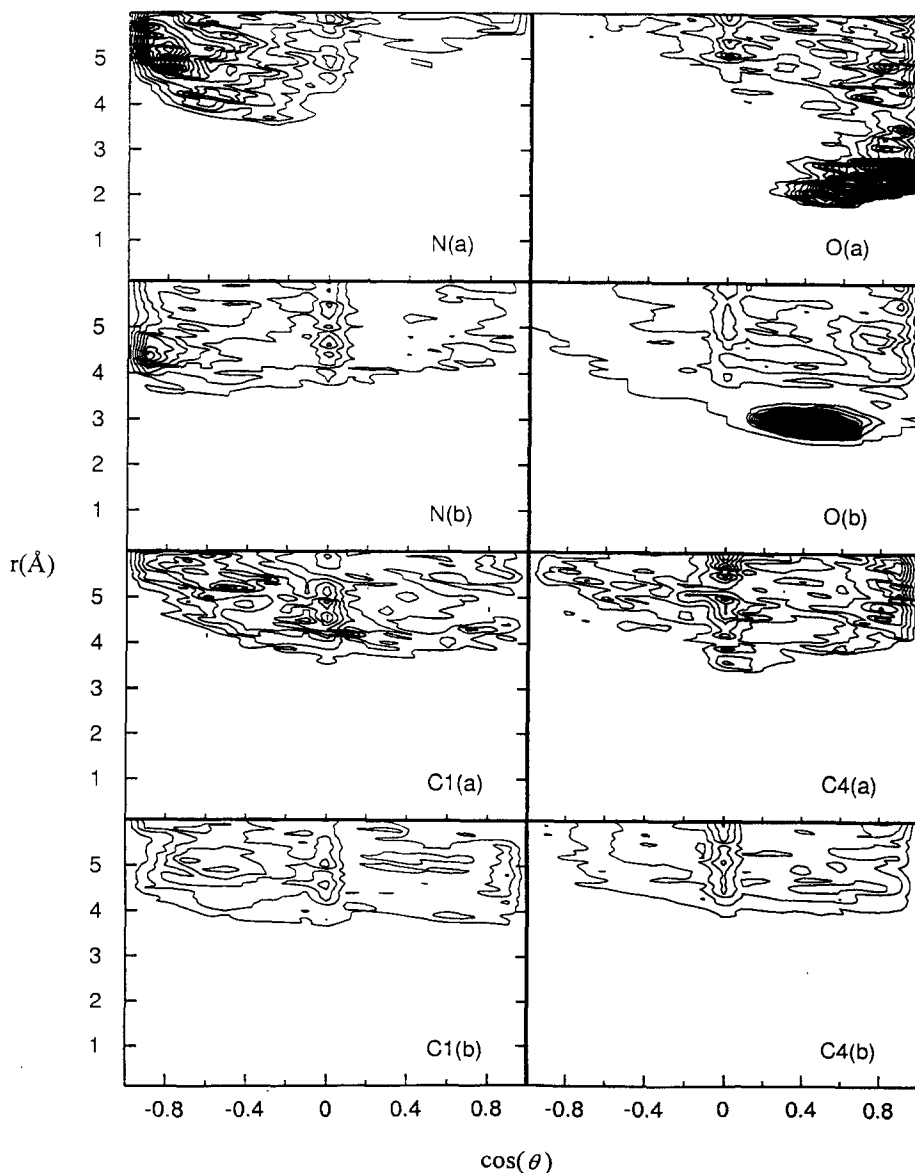


Fig. 5. Contour plots of the radial-angular distribution functions $f(r, \theta)$ of (a) acetone and (b) methanol dipoles around some zwitterion atoms.

Table 3

Wavelength (λ) of the transition with the highest oscillation strength obtained using different levels of solvent representation

		λ (nm)		
		quinone	zwitterion	experimental
In vacuo		451.04	545.96	–
SCRF approach	acetone	458.60	550.13	–
	methanol	458.85	550.18	–
QM/MM mixed model	acetone	476.21	525.13	–
	methanol	473.73	525.67	–
Supermolecule model	acetone	493.83	655.74	–
	methanol	481.93	533.33	–
		acetone	–	585.00
		methanol	–	483.00

In the case of the supermolecule model, the maxima of the spectra are used (see Fig. 6).

differences between SCRF and in vacuo results are small is not unexpected, since MC's shape is far from spherical. However, as we will see later, the zwitterion's main site of interaction with the solvent is the O atom that is closer to the dielectric sphere than the rest of the atoms. Table 3 also shows that the QM/MM mixed model does not produce a significant spectrum perturbation. Similar results were obtained either for configurations obtained from the MD, or for energy minimized ones. Even though a large change in the dipole moment of MC's zwitterion upon excitation was observed this has no effect on the solvatochromism, since the dipole moments of both solvents are similar, and therefore they have similar non-specific effects on the solvatochromism, as evidenced by the LSER π^* values. Although the QM/MM model reproduces well the specific and non-specific MC(ground state)/solvent interactions for the sake of the MD calculation, it is unable to account properly for specific effects on the electronic spectra. This model neglects possible MC–solvent charge transfer interactions by making their atomic orbitals orthogonal to each other. As we will see next, these interactions are the key to explain the solvatochromism.

In the supermolecule approach, the first solvation shell is included explicitly in the quantum mechanical calculation. The effect of the bulk on the

solute–solvent supermolecule is taken care of by the inclusion of an SCRF field. In Fig. 6 we show the absorption spectra calculated using this method. Table 3 shows that if the zwitterion predominates over the quinone, the calculations predict a solvent shift of 3610 cm^{-1} , in remarkable agreement with the experimental value of 3500 cm^{-1} . The relative predominance of the zwitterion over the quinone is supported by the results of Luzhkov and Warshel [11], as well as and with the early arguments regarding the relative zwitterion/quinone stability of Brooker et al. [2].

To further study the relative zwitterion predominance, we calculated the supermolecule's total energy (electronic energy + nuclear repulsion energy) using AM1. While in vacuo the quinone structure is 25.73 kcal/mol more stable than the zwitterion, the opposite is true for the solvated structures in both solvents. The zwitterion–solvent supermolecule is more stable than the quinone–solvent supermolecule by $105.39 \pm 44.10\text{ kcal/mol}$ in methanol and by $12.40 \pm 77.49\text{ kcal/mol}$ in acetone. In spite of their large uncertainties these energies show a clear stabilization of the zwitterion with respect to the quinone in both solvents.

We will now analyse with more detail the electronic transition responsible of the solvatochromism. The changes in the supermolecule's AO Mulliken populations [30] during the electronic transitions close to the maximum of the absorption spectra reveal that they are HOMO–LUMO π – π^* transitions for the four systems. In Table 4 we show the electron transfer from the N half of MC to the O half during the electronic transition. We see from this table that

Table 4

Charge transfer between the left- and right-hand sides of MC:

$$\sum_{\mu} \Delta MP_{\mu} - \sum_{\nu} \Delta MP_{\nu},$$

with $\mu \in$ left-hand side of the C2–C3 bond (O-half) and $\nu \in$ right-hand side (N-half); ΔMP_x is the difference in Mulliken populations between the excited and fundamental MC states for atomic orbital x

	Quinone	Zwitterion
Acetone	0.147 ± 0.016	-0.345 ± 0.080
Methanol	0.128 ± 0.002	-0.765 ± 0.0004

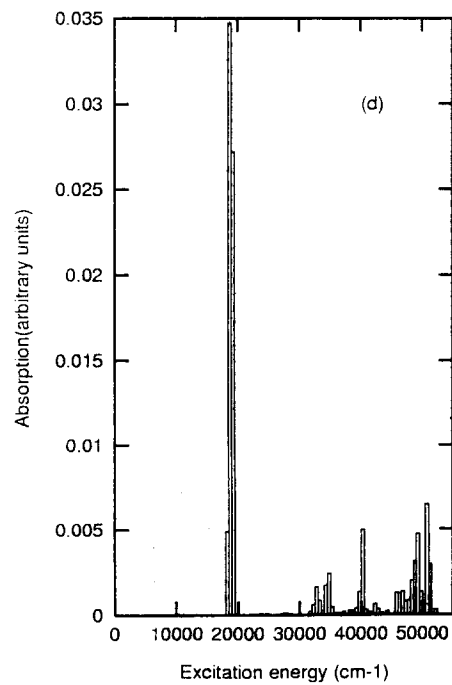
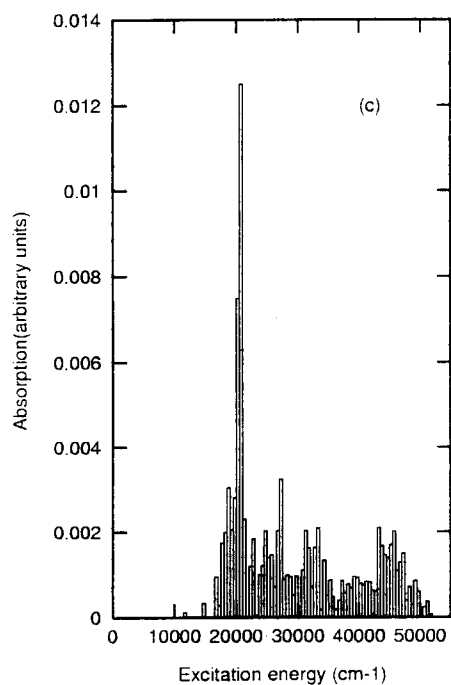
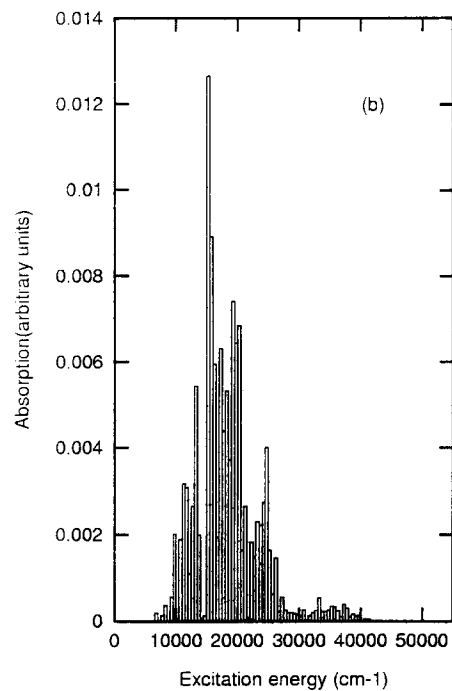
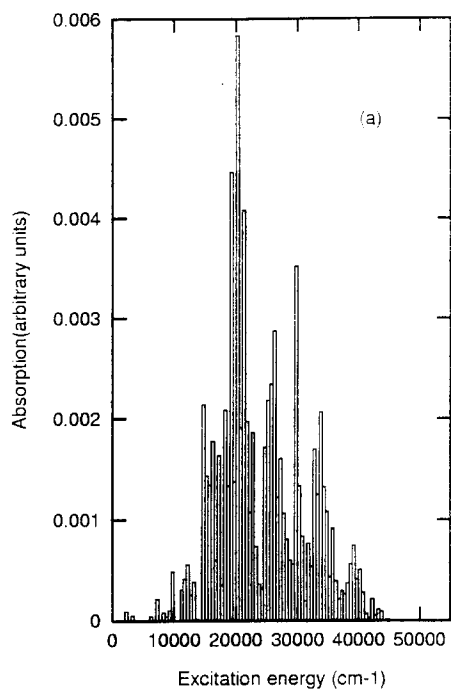


Table 5

Solute/solvent charge transfer:

$$\sum_{\mu} \text{MP}_{\mu}^{\text{exc}} - \sum_{\mu} \text{MP}_{\mu}^{\text{fund}},$$

where $\text{MP}_{\mu}^{\text{exc}}$ and $\text{MP}_{\mu}^{\text{fund}}$ are the Mulliken populations of atomic orbital μ in the excited and fundamental states of MC, respectively

	Quinone	Zwitterion
Acetone	0.028 ± 0.021	0.101 ± 0.264
Methanol	0.017 ± 0.010	0.027 ± 0.015

for the quinone the electron transfer is in the $\text{N} \rightarrow \text{O}$ direction, whereas the opposite is true for the zwitterion. This agrees with the idea of a π -electron transfer from the donor oxygen to the acceptor quaternary nitrogen in the zwitterion and from donor nitrogen to the carbonyl oxygen in the quinone.

Table 5 shows the electron transfer from solvent to solute. We see that in all cases there is charge transfer from solvent to solute, this being much larger for the zwitterion–acetone case than for the others. We think this could be the main cause of the failure of the QM/MM mixed model in the prediction of MC's solvatochromism. The usefulness of the consideration of the solvent/solute charge transfer to reproduce the correct solvent shift was well demonstrated for other systems [31]. We have studied the average localization of those solvent molecules that show a variation of their total electronic populations during the electronic transitions. For the quinone we found that they are located around the atoms C1 and C4 either in methanol or acetone. For the zwitterion, on the other hand, they are near O(MC) in both solvents. In acetone, the closest solvent molecule has its center of mass at 2.4 ± 0.3 Å from O(MC), and its dipole forms an angle θ of $38.4 \pm 10.0^\circ$. This clear orientation would be due to a nucleophile–carbonyl interaction between O(MC) and acetone. In methanol, the closest H(Met) is at 1.6 ± 0.1 Å from O(MC) and forms an angle O(Met)–H(Met)–O(MC) of $172.4 \pm 4.5^\circ$. Therefore, the O atom of the zwitterion forms a hydrogen bond with methanol.

4. Conclusions

We studied the solvatochromism of a strongly polar merocyanine dye (MC) by performing semiempirical electronic structure calculations on solute–solvent systems using different levels of solvent representation. Where it was needed, the solvent configurations around the solute were obtained from molecular dynamics simulations in which a quantum mechanics–molecular mechanics (QM/MM) mixed field was used. The present calculations predict a shift of the absorption band of MC between methanol and acetone of 3610 cm^{-1} , in remarkable agreement with the experimental value of 3500 cm^{-1} .

The quinone and zwitterion resonance forms of the solute were studied. The solvents used are very similar in their non-specific effects, and therefore their solvatochromic effect is expected to arise mainly from specific interactions. Accordingly, we found that the solvents have to be included explicitly in the electronic structure calculation to account for the solvatochromism. Methods in which the solvent is replaced by a continuum or where solvent charges are introduced into effective solute Hamiltonians failed completely to predict the experimental shift. We found that the band shift would be produced by the effect of the first solvation shell over the zwitterion valence structure, that predominates in both solvents. A nucleophile–carbonyl interaction in acetone and a hydrogen bond in methanol would be the main causes of the solvatochromism.

Finally, we should note that the method could be much improved, for example by incorporating the first solvation shell in the QM region of the QM/MM molecular dynamics simulation. Besides, for the sake of computational efficiency we performed our MD simulations on fixed geometry zwitterion and quinone forms of MC. In a more realistic, but expensive, study one should take into account that the actual solute contains contributions of both zwitterion and quinone. Also, the geometry variations along the MD run should be included. However, and even though more solvents and solutes should be studied, the

Fig. 6. Calculated absorption spectra for (a) quinone in acetone, (b) zwitterion in acetone, (c) quinone in methanol, and (d) zwitterion in methanol. Each bar represents the relative number of MD configurations having a value of the transition energy within an interval of 500 cm^{-1} , multiplied by the mean oscillator strength.

present results are very encouraging and suggest that this method is a good one to study the solvatochromism of merocyanines.

Acknowledgements

We are very grateful with María Silvina Fornasari, Diana Roncaglia, and Oscar Ventura for useful discussions. Financial support from the Fundación Antorchas and the Universidad Nacional de Quilmes is gratefully acknowledged.

References

- [1] L.G.S. Brooker, G.H. Keyes, R.H. Sprague, R.H. VanDyke, E. VanLare, G. VanZandt, F.L. White, H.W.J. Cressman, S.G. Dent, *J. Am. Chem. Soc.* 73 (1951) 5332.
- [2] L.G.S. Brooker, G.H. Keyes, D.W. Heseltine, *J. Am. Chem. Soc.* 73 (1951) 5350.
- [3] J. Catalán, E. Mena, W. Meutermans, J. Elguero, *J. Phys. Chem.* 96 (1992) 3615.
- [4] C. Reichardt, *Solvent Effects in Organic Chemistry*, Verlag Chemie, Weinheim, New York, 1979, p.194.
- [5] H.G. Benson, J.N. Murrell, *J. Chem. Soc., Faraday Trans. 2* 68 (1972) 137.
- [6] A. Botrel, A. LeBeuze, P. Jacques, H. Strub, *J. Chem. Soc., Faraday Trans. 2* 80 (1984) 1235.
- [7] I.D.L. Albert, T.J. Marks, M.A. Ratner, *J. Phys. Chem.* 100 (1996) 9714.
- [8] J.O. Morley, *J. Mol. Struct. (Theochem)* 304 (1994) 191.
- [9] R. Constanciel, O. Tapia, *Theor. Chim. Acta* 48 (1978) 75.
- [10] M.M. Karelson, M.C. Zerner, *J. Phys. Chem.* 96 (1992) 6949.
- [11] V. Luzhkov, A. Warshel, *J. Am. Chem. Soc.* 113 (1991) 4491.
- [12] P. Jacques, *J. Phys. Chem.* 90 (1986) 5535.
- [13] C. Reichardt, *Chem. Rev.* 94 (1994) 2319.
- [14] W.L. Jorgensen, J. Tirado-Rives, *J. Am. Chem. Soc.* 110 (1988) 1657.
- [15] S.J. Weiner, P.A. Kollman, D.A. Case, U.C. Singh, C. Ghio, G. Alagona, S. Profeta, P. Weiner, *J. Am. Chem. Soc.* 106 (1984) 765.
- [16] W.L. Jorgensen, *J. Phys. Chem.* 90 (1986) 1276.
- [17] W.L. Jorgensen, J.M. Briggs, M.L. Contreras, *J. Phys. Chem.* 94 (1990) 1683.
- [18] R.C. Willhoit, B.J. Zwolinski, *J. Phys. Chem. Ref. Data, Suppl.* 1 (1973) 2.
- [19] TRC Thermodynamic Tables: Non-Hydrocarbons; table 23-2-1-(1.1130)-a, Texas A&M University System, College Station, TX, 1965, p.A-5370.
- [20] H.J.C. Berendsen, J.P.M. Postma, W.F. van Gunsteren, A. DiNola, J.R. Haak, *J. Chem. Phys.* 81 (1984) 3684.
- [21] M.J.S. Dewar, E.G. Zoebisch, E.F. Healy, J.J.P. Stewart, *J. Am. Chem. Soc.* 107 (1985) 3902.
- [22] J.J.P. Stewart, in: K.B. Lipkowitz, D.B. Boyd (Eds.), *Reviews in Computational Chemistry*, vol. 1, VCH Publishers, New York, 1990, p.45.
- [23] This treatment is implemented in the Hyperchem Program Package.
- [24] J. Ridley, M.C. Zerner, *Theor. Chim. Acta* 32 (1973) 111.
- [25] J. Ridley, M.C. Zerner, *Theor. Chim. Acta* 42 (1976) 223.
- [26] A.D. Bacon, M.C. Zerner, *Theor. Chim. Acta* 53 (1979) 21.
- [27] M.C. Zerner, G.H. Loew, R.F. Kirchner, U.T. Mueller-Westhoff, *J. Am. Chem. Soc.* 102 (1980) 589.
- [28] M. Ferrario, M. Haughney, I.R. McDonald, M.L. Klein, *J. Chem. Phys.* 93 (1990) 5156.
- [29] M. Haughney, M. Ferrario, I.R. McDonald, *J. Phys. Chem.* 91 (1987) 4934.
- [30] R.S. Mulliken, *J. Chem. Phys.* 23 (1955) 1833.
- [31] K.K. Stavrev, M.C. Zerner, T. Meyer, *J. Am. Chem. Soc.* 117 (1995) 8684.